HHS Public Access

Author manuscript

J Vis Exp. Author manuscript; available in PMC 2019 March 14.

Measurement of energy metabolism in explanted retinal tissue using extracellular flux analysis.

Jeffrey R. Millman[1,2], **Teresa Doggett**[3], **Christina Oberlin**[3], **Sheng Zhang**[3], **Clay F. Semenkovich**[1], and **Rithwick Rajagopal**[3]

Jeffrey R. Millman: jmillman@wustl.edu; Teresa Doggett: doggettta@wustl.edu; Christina Oberlin: oberlin.christina@wustl.edu; Sheng Zhang: zhangsheng@wustl.edu; Clay F. Semenkovich: csemenko@wust.edu; Rithwick Rajagopal: rajagopalr@wustl.edu

[1]Division of Metabolism, Endocrinology and Lipid Research, Department of Medicine, Washington University School of Medicine, Saint Louis, MO, USA

[2]Department of Biomedical Engineering, Washington University in Saint Louis, Saint Louis, MO, USA

[3]Department of Ophthalmology and Visual Science, Washington University School of Medicine, Saint Louis, MO, USA

LONG ABSTRACT:

High acuity vision is a heavily energy-consuming process, and the retina has developed several unique adaptations to precisely meet such demands while maintaining transparency of the visual axis. Perturbations to this delicate balance cause blinding illnesses, such as diabetic retinopathy. Therefore, the understanding of energy metabolism changes in the retina during disease is imperative to the development of rational therapies for various causes of vison loss. The recent advent of commercially-available extracellular flux analyzers has made the study of retinal energy metabolism more accessible. This protocol describes the use of such an analyzer to measure contributions to retinal energy supply through its two principle arms – oxidative phosphorylation and glycolysis – by quantifying changes in oxygen consumption rates (OCR) and extracellular acidification rates (ECAR) as proxies for these pathways. This technique is readily performed in explanted retinal tissue, facilitating assessment of responses to multiple pharmacologic agents in a single experiment. Metabolic signatures in retinas from animals lacking rod photoreceptor signaling are compared to wild-type controls using this method. A major limitation in this technique is the lack of ability to discriminate between light-adapted and dark-adapted energy utilization, an important physiologic consideration in retinal tissue.

SHORT ABSTRACT:

This technique describes real time recording of oxygen consumption and extracellular acidification rates in explanted mouse retinal tissues using an extracellular flux analyzer.

Corresponding Author: Rithwick Rajagopal, Tel: (314)-362-6929.

DISCLOSURES:
The authors have nothing to disclose.

Keywords

Retina; oxygen consumption rate; extracellular acidification rate; oxidative phosphorylation; glycolysis; mitochondria; metabolism

INTRODUCTION:

The retina is among the most energy-demanding tissues in the central nervous system[1]. Like most tissues, it generates adenosine triphosphate (ATP) *via* glycolysis in the cytosol or *via* oxidative phosphorylation in mitochondria. The energetic advantage of oxidative phosphorylation over glycolysis to produce ATP from one molecule of glucose is clear: 36 molecules of ATP generated from the former vs 2 molecules of ATP generated from the latter. Accordingly, retinal neurons primarily depend on mitochondrial respiration for energy supply and this is reflected by their high density of mitochondria[2]. Yet, the retina also relies heavily on glycolytic machinery even when oxygen is abundant. This process of aerobic glycolysis was originally described in cancer cells by Otto Warburg[3], who once noted that the retina was the only post-mitotic tissue capable of this form of metabolism[4]. Since those initial observations, many post-mitotic tissues have been described to engage in varying degrees of glycolysis in additional to oxidative phosphorylation to meet their ATP demands.

Phototransduction, visual pigment recycling, biosynthesis of photoreceptor outer segments, and synaptic activity are all energy demanding processes in photoreceptors, the predominant neuronal subclass in the retina. But the need to actively transport ions against their electrical and concentration gradients is by far the most energetically consuming process in neurons[1]. Photoreceptors are peculiar neurons in the sense that they are depolarized in the absence of stimulation (*i.e.*, in the dark), whereas a light stimulus triggers channel closure and subsequent hyperpolarization. Therefore, in the dark, the retina consumes large quantities of ATP to maintain its depolarization or “dark current” as it is commonly called. From an adaptive standpoint, a major challenge in supplying these vast quantities of ATP is the need for organisms to maintain visual clarity through the optical axis. The inverted retinal architecture seen in modern creatures is the dominant solution, as it keeps the dense capillary network supplying photoreceptors away from the path of light. But this marvel of natural bioengineering places the retina at a precipice in terms of metabolic reserve. Even small insults to retina can potentially disrupt the delicate balance of energy supply to demand, and visual dysfunction or frank blindness may ensue quickly.

Given the unique energetic demands of the neural retina, coupled with its tight restriction of vascular supply, accurate measurement of ATP consumption in the retina and its changes during disease could have profound implications in understanding and treating blinding conditions such as retinitis pigmentosa and diabetic retinopathy. Traditionally, these measurements require costly, custom-designed equipment with most studies emerging from a handful of laboratories entirely dedicated to measurements of metabolic activity[2,5–8].

Techniques include individual assays for specific metabolites, tracer studies using radio-labeled precursors, oxygen consumption recording using Clark electrodes, and metabolomics profiling[9]. With advances in high-throughput technology and increased

availability of commercial devices, techniques to record retinal metabolism are increasingly accessible and affordable. The method described here measures both oxidative phosphorylation and glycolysis in retina using explanted tissue and a commercially-available extracellular flux analyzer[9–12]. This analyzer separately records oxygen consumption rates (OCR) and the extracellular acidification rate (ECAR), serving as indirect indicators of oxidative phosphorylation and glycolysis, respectively[13].

These measurements are done by a probe submersed within a microchamber created over the tissue of interest. This adaptation of previously published methods uses a capture plate originally designed for pancreatic Islets of Langerhans to record metabolic activity in small, circular sections of mouse retina. Multiple pharmacologic exposures can be delivered to the tissue during the course of a single recording because the system contains 4 injections ports for each sample well. Using this system with separate protocols optimized for ECAR and OCR recordings, the responses of wild-type retinas can be compared to retinas lacking *transducin* (*Gnat1*$^{-/-}$), a cause of congenital stationary night blindness in humans[14].

PROTOCOL: (Instructions)

Protocols followed the Association for Research in Vision and Ophthalmology Statement for the Use of Animals and were approved by Washington University.

1. Animals:

1.1. Keep animals in standard housing with a 12 hours dark to 12 hours light cycle. Begin experiments at standardized times to avoid circadian effects, typically in the morning shortly after lights are turned on.

2. Solutions

2.1. Prepare base media by dissolving 8.4 mg of powdered media in double-distilled H_20, and adjust pH to 7.4 with either HCl or NaOH, to final volume of 1 L. Filter sterilize this solution with a 0.22 μm tissue culture filter.

2.1.2. Add 1 M glucose and 100 mM sodium pyruvate to the media to achieve final concentration of 5 mM glucose and 1 mM pyruvate.

2.1.3. Place a 50 mL aliquot of the base media in a 37 °C water bath.

2.2. Prepare lysis solution, for tissue quantitation at the end of the flux analysis, by adding tris base to 10 mM, polyethylene glycol tert-octylphenyl ether to 0.2% (v/v), and EDTA to 1 mM, all in ddH20. Mix until all components completely dissolved and adjust pH to 8.0.

2.3. For mitochondrial stress protocol prepare an 11 μM stock of oligomycin, an ATP Synthase inhibitor, dissolved in base media to target a final concentration of 1 μM in the well. Prepare an 11 μM stock of FCCP, an uncoupling agent, dissolved in base media to target a final concentration of 1 μM in the well. Prepare a cocktail of the electron transport chain inhibitors, rotenone and antimycin A (RAA) by adding rotenone to 11 μM and

antimycin A to 22 μM, dissolved in base media to target a final concentration of 1 μM rotenone and 2 μM antimycin A in the well.

2.3.2. For glycolysis protocol prepare a 220 mM stock of glucose dissolved in base media, to target a final concentration in well is 20 mM. Also prepare a 1.1 M stock of 2-Deoxyglucose (2-DG), a competitive inhibitor of glucose and glycolytic antagonist, by dissolving it in base media. This will target a final concentration of 100 mM 2-DG in the well.

3. To calibrate the instrumentation for an extracellular flux assay, add 1 mL calibration solution to each well of the sensor cartridge (24 wells total) and incubate at 37 °C in a CO_2-free incubator overnight (or at least 8 h.).

3.1. Load additives for the mitochondrial stress protocol or the glycolysis protocol into each injector port, A through D, on the sensor cartridge, adjusting for volume changes in the well.

Note: As an example, a typical assay would include 45 μL into the first injector port, 49.5 μL into the second, 54.5 μL into the third and 60 μL into the last, assuming an initial well volume of 450 μL.

3.2. During the first several experiments, load base media into port A to gauge how much tissue movement/artefact occurs after a port injection.

3.2. Allow the loaded sensor plate to incubate at 37 °C in a non-CO_2 incubator for at least 60 minutes.

4. Isolation of fresh mouse retinal tissue, adapted from the technique of Dr. Barry Winkler[15].

4.1. After administering deep anesthesia using a standard ketamine/xylazine cocktail, euthanize mice by cervical dislocation.

4.2. Use a medium-sized curved forceps to grasp the posterior globe at the optic nerve and gently apply forward pressure to proptose the eye (Figure 1A).

4.2.1. With a clean razor blade, create a limbus to limbus incision across the cornea using a single, deliberate pass of the blade.

4.2.2. Using fine, angled McPherson-style forceps, pinch the posterior globe to express the lens and anterior hyaloid membranes out of the corneal incision. Discard these tissues.

4.2.3. Repeat the pinching maneuver with forceps to express the neural retina.

4.2.4 Using the forceps like a spoon to lift the retina, rather than to grasp the tissue, transfer the retina away from the corneal incision and place directly into warm media in a 3 cm dish or a 6-well tissue culture cluster plate.

4.3. Use 2 fine, angled McPherson-style forceps to gently dissect remaining vitreous from the retina. This is best done by grasping the vitreous at the periphery of the retinal cup and pulling towards the center, with a final disinsertion of the vitreous body from the center as a

whole. Using the forceps, remove any residual retinal pigment epithelium from the photoreceptor surface of the retina.

4.3.1. Cut a P1000 pipet tip with a razor blade to create a ~4 mm opening to prevent undue trauma to the delicate retinal tissue during transfer maneuvers.

4.3.2. Transfer the isolated retinal tissue into fresh media using a cut P1000 pipet tip.

4.3.3. Cut 1 mm punches of retina around the optic nerve with a 1 mm biopsy punch equipped with a plunger to dislodge the tissue in case it becomes lodged into the bore (Figure 1B). Set the retinal punches aside in clean media kept on a 37°C block or heating pad.

5. Assay protocol

5.1. Transfer individual punches to a 24-well islet capture microplate using a cut P1000 tip, aspirating 450 μL of media along with the tissue.

5.2. Use fine, straight forceps to gently manipulate punches into the center of the microplate. Keep punches orientated in the same direction (*e.g.,* ganglion cell side upwards).

5.2.1. Rest the capture plate on a heating pad or heating block set to 37 °C as these steps are repeated for the remaining samples.

Note: For each experiment, set aside 3–4 blank wells with 450 μL of base media to serve as negative controls. In the remaining 20–21 wells, test each biologic replicate in triplicate.

Therefore, each 24-well plate will allow for recording from 6–7 different animals or treatment conditions.

5.3. Avoiding air bubbles, gently position the islet capture mesh inserts into each well using forceps and secure the inserts with a metal plunger, or with a cut P1000 pipet tip (Figure 1C).

Note: Avoid excessive tissue movement during this step, to maintain retinal punch position within the center of the sample microchamber. Air bubbles severely distort OCR readings.

Although the microchamber has adequate depth to accommodate typical mouse retina (Figure 1C), occasionally machining-defects in the mesh inserts may cause tissues to become overly compressed during screen insertion. If this happens, simply make a note of the crushed tissue and exclude that sample from the final analysis.

5.4. Incubate the tissue plate in a 37 °C CO_2-free incubator for at least 60 minutes.

5.5. Program the extracellular flux analyzer using Mix, Wait, Measure and Repeat commands. As an example, a typical experiment with retinal tissue may include the following:

Step 1: Mix 2 minutes

Step 2: Wait 2 minutes

Step 3: Measure 5 minutes

Repeat steps 1–3 between 5–8 times (cycles) for a baseline recording, and after injection of each compound being tested during the run.

5.6. Press the program START button on the extracellular flux analyzer and follow the instructions on the screen to insert the sensor cartridge for calibration.

5.7. At the end of the calibration, follow instructions on the screen to replace the calibrant plate with the plate containing the retinal samples.

5.8. Allow the program to run, as programmed.

5.9. At the completion of the run, follow instructions on the screen to eject the tissue plate.

5.10. View the results of the run and store the data file.

5.11. With a bent 20 gauge needle and forceps, remove all mesh inserts from the wells, leaving the retinal punch behind.

5.12. Carefully aspirate the media from the tissue and wash the tissue twice with 0.5 mL cold PBS. Aspirate the PBS after washing.

5.13. Add 100 μL of lysis buffer to each well and pipet up and down to homogenize tissue.

5.14 Quantitate input levels based on total double-stranded DNA (dsDNA) or total protein content

Note: The following is based on a commercially available dsDNA assay:

5.15. Dilute lysed samples 1:1 by adding 100 μL TE buffer, and transfer 100 μL of the diluted sample to a 96 well plate.

5.15.1. Add 100 μL detection buffer into each well. After mixing 2–5 minutes, quantitate fluorescence after excitation at 480 nm and emission at 520 nm, comparing to a standard curve.

5.15.2. Normalize the raw extracellular flux tracing to DNA content within the well.

Note: In the results presented here, samples are normalized to 50 ng dsDNA – a typical amount in a 1 mm retinal punch. Therefore, absolute values presented here may be compared to papers presenting data “per retinal punch”. Normalize tracings to an internal standard, such as the baseline run at 5 mM glucose concentration.

REPRESENTATIVE RESULTS:

Using the described techniques (summarized in Figure 1), retinal explants from 8 week-old wild type mice were compared to age- and background- matched *transducin* null mice (*Gnat1*$^{-/-}$). Because *Gnat*$^{-/-}$ animals lack the machinery to close cyclic-nucleotide gated ion

channels in response to light stimuli, their rod photoreceptors remain depolarized even in light[14]. The subsequent need to maintain potassium efflux would create a large ATP demand, resulting in bioenergetic strain. To determine if such shifts in energy demands would increase oxidative phosphorylation or glycolytic flux, tissues from wild type mice and *Gnat1*$^{-/-}$ mice were compared using the extracellular flux analyzer. At baseline, in the presence of 5 mM glucose and 1 mM pyruvate, retinal tissues from wild-type animals have similar rates of acid efflux compared to *Gnat1*$^{-/-}$ mutants. Similar patterns are seen after addition of 20 mM glucose and the glycolytic inhibitor 2-DG (Figure 2A). These data may also be mathematically transformed to represent fractional changes from baseline (Figure 2B), a format which may allow for better comparison between different experimental interventions.

Absolute OCR at baseline is equivalent between WT and mutant retinal tissue (Figure 3A). The addition of 20 mM glucose increases mitochondrial respiration, but no change is observed between groups in terms of absolute quantification or in terms of change from baseline (Figure 3B). The addition of 1mM FCCP (an uncoupling agent) to demonstrate maximal mitochondrial respiratory rates does not significantly increase OCR above the level seen with high glucose in WT or *Gnat1*$^{-/-}$ tissues. However, signals from both mice drastically drop after the addition of RAA cocktail.

Ideally, extracellular flux experiments run in the presence of the ATP synthase inhibitor oligomycin aid in identifying sources of proton leak, occurring when movement through the electron transport chain is not associated with ATP production[16]. In retinal explants from 8 week-old C57BL/6J mice, oligomycin treatment robustly lowers OCR, as expected (Figure 4). But subsequent addition of FCCP, to find maximal OCR, only nominally increases the OCR to about 60% of baseline, consistent with a prior study[11].

The XF24 analyzer uses submersible probes that make a tight seal within the tissue well, creating a transient microenvironment for measurement of oxygen and acid flux. Positioning of retinal tissue in the well plate (in relation to the sensors) could potentially influence OCR recordings, and lead to unwanted confounders, and some have advocated placing retinal tissue directly underneath the oxygen sensor with the photoreceptor outer segments oriented toward the sensor[11]. To test the effects of retinal tissue position on OCR measurements, tissues from young C57BL/6J mice (8 weeks old) were analyzed in two orientations: retinal ganglion cells facing down onto the plate (*i.e.*, photoreceptors placed upright closest to sensor); or facing up toward the sensor. No differences in relative OCR in response to FCCP or RAA were observed, indicating equivalent sensitivity for maximal and minimal mitochondrial respiratory rates in either orientation (Figure 5A). In addition, absolute OCR measurements were also equivalent between retinal tissues in either orientation (Figure 5B).

DISCUSSION:

OCR and ECAR are readily measured in explanted retinal tissue using the XF24 bioanalyzer using the described techniques. This method departs from those of other groups in several critical steps. Retinal tissues are isolated though a large corneal incision without enucleating the globe, as originally described by Winkler[15]. This method of retinal isolation allows for a

rapid transfer from the living eye into the tissue capture plate (often under 5 minutes). Tissues are kept at 37 °C throughout the process, which preserves cellular respiration better than when they are placed on ice. Media with minimal additives are used for initial measurements, omitting any buffering agents such as HEPES or sodium bicarbonate, serum, or excess macronutrients, as this allows for more reliable measurements of basal energy 24-well format, rather than in 96-wells, to minimize trauma to the tissue. Retinal tissue is placed in the center of the well, within the tissue microchamber, and secured with a mesh insert. Doing so allows for accurate recording of ECAR and OCR, while preventing excessive tissue movement during the run, and eliminates the need for other reagents such as tissue adhesives. A vehicle injection during the run is recommended, especially when setting up recording experiments for the first time, as this will provide a sense of how well the tissue is secured within the capture plate. OCR recordings using this technique are independent of retinal orientation within the well, but the orientation must be kept consistent among samples within experiments. All measurements are taken only after retinal metabolism has reached steady-state following injection of test compounds.

This protocol describes normalization of data to total DNA content, as a proxy for cell number. Such a technique is advantageous because it will account for changes to cell number driven by variation in retinal thickness, punch size, or differences in cellularity between genetically dissimilar samples. Total protein-based normalization is also a reliable method, and has the advantage of minimizing differences in total mitochondrial mass between retinal samples. However, normalization based on protein content in whole tissue may be confounded by changes in extracellular matrix between samples. Normalization of flux recordings to the baseline, as shown in the representative results, is advantageous because it minimizes variability in retinal punch size between replicates and easily allows interpretation of changes due to pharmacologic interventions. However, reporting of raw values allows for better comparison between different experiments and for experiments performed using different flux recording methods.

Results using these techniques are comparable to those reported elsewhere. Though oligomycin – an ATP synthase inhibitor – is typically used to measure proton leak within tissues or cells of interest, this compound has untoward effects on retinal metabolism. In the experiments reported here, a 60% decrease in maximal retinal OCR elicited by FCCP is observed after exposure to oligomycin (Figure 4), nearly identical to a previous study[11]. A potential explanation for this finding is irreversible damage or modification to retinal mitochondria by ATP synthase inhibition. Furthermore, as Kooragayala and colleagues first reported[11], retinal mitochondria are likely operating at near maximal rates in basal conditions since an electron transport chain uncoupling agent, FCCP, only increases OCR by about 15% (Figure 3, Figure 5). Extracellular flux recordings in explanted retinal tissues demonstrate a large reserve glycolytic capacity, since the addition of 20 mM glucose elicits a two-fold increase in ECAR (Figure 2).

Because oligomycin, usually used to gauge maximal glycolytic capacity, has deleterious effects in retinal tissue (Figure 4) the use of high glucose addition to the recording may serve as better proxy to gauge glycolytic reserve in the retina. An important caveat preventing the use of ECAR as a pure proxy for glycolytic rate is that CO_2 liberated by the citric acid cycle

can be a significant source of acid in cultured tissue[17]. Excess pyruvate does not increase ECAR above the levels elicited by high glucose, and glycolytic flux is nearly eliminated in retinal explants using excess molar ratios of 2-DG (Figure 2). Since ATP is used to regenerate membrane potential occurring from depolarization events in the dark-adapted retina, animals lacking *transducin* were expected to expend more energy than WT counterparts. However, in explants, differences in retinal energy metabolism between *Gnat1*$^{-/-}$ and controls were not seen in the experiments described here (Figures 2 and 3). These results are consistent with those obtained using a custom perfusion apparatus to measure OCR in *Gnat1*$^{-/-}$ animals[18]. Notably, the custom apparatus used by Du and colleagues allowed for measurement of OCR under light-adapted and dark adapted conditions. By doing so, a small but significant decrease in OCR after light exposure is detected in wild-type retinas, but not in *Gnat1*$^{-/-}$ retinas[18]. This illustrates a major limitation of the current technique in measuring ECAR and OCR in explanted retinas – the extracellular flux analyzer used here relies on visible light excitation of fluorophores embedded in its oxygen and pH sensors, eliminating the possibility of performing measurements in dark- adapted tissues. Such measurements are highly relevant to visual physiology and will still require the use of older techniques designed exclusively for the study of retinal metabolism.

ACKNOWLEDGMENTS:

We thank Dr. Alexander Kolesnikov and Dr. Vladimir Kefalov for providing *Gnat1*$^{-/-}$ mice, for helpful feedback and advice, and for reading the manuscript.

This work was supported by NIH EY025269 (RR), the Diabetes Research Center at Washington University - NIH DK020579 (JRM and RR), a Career Development Award from Research to Prevent Blindness (RR), the Horncrest Foundation (RR), a Career Development Award from JDRF (JRM), NIH DK101392 (CFS), DK020579 (CFS), DK056341 (CFS), and DK114233 (JRM).

REFERENCES:

1. Wong-Riley MT Energy metabolism of the visual system. Eye and brain. 2 99–116, (2010). [PubMed: 23226947]
2. Ames A, 3rd, Li YY, Heher EC & Kimble CR Energy metabolism of rabbit retina as related to function: high cost of Na+ transport. The Journal of neuroscience : the official journal of the Society for Neuroscience. 12 (3), 840–853, (1992). [PubMed: 1312136]
3. Warburg O On the origin of cancer cells. Science. 123 (3191), 309–314, (1956). [PubMed: 13298683]
4. Wubben TJ et al. Photoreceptor metabolic reprogramming provides survival advantage in acute stress while causing chronic degeneration. Scientific reports. 7 (1), 17863, (2017). [PubMed: 29259242]
5. Du J, Linton JD & Hurley JB Probing Metabolism in the Intact Retina Using Stable Isotope Tracers. Methods in enzymology. 561 149–170, (2015). [PubMed: 26358904]
6. Felder AE, Wanek J, Tan MR, Blair NP & Shahidi M A Method for Combined Retinal Vascular and Tissue Oxygen Tension Imaging. Scientific reports. 7 (1), 10622, (2017). [PubMed: 28878307]
7. Hurley JB, Lindsay KJ & Du J Glucose, lactate, and shuttling of metabolites in vertebrate retinas. Journal of neuroscience research. 93 (7), 1079–1092, (2015). [PubMed: 25801286]
8. Winkler BS Glycolytic and oxidative metabolism in relation to retinal function. The Journal of general physiology. 77 (6), 667–692, (1981). [PubMed: 6267165]

9. Pelletier M, Billingham LK, Ramaswamy M & Siegel RM Extracellular flux analysis to monitor glycolytic rates and mitochondrial oxygen consumption. Methods in enzymology. 542 125–149, (2014). [PubMed: 24862264]
10. Joyal JS et al. Retinal lipid and glucose metabolism dictates angiogenesis through the lipid sensor Ffar1. Nature medicine. 22 (4), 439–445, (2016).
11. Kooragayala K et al. Quantification of Oxygen Consumption in Retina Ex Vivo Demonstrates Limited Reserve Capacity of Photoreceptor Mitochondria. Investigative ophthalmology & visual science. 56 (13), 8428–8436, (2015). [PubMed: 26747773]
12. Pearsall EA et al. PPARalpha is essential for retinal lipid metabolism and neuronal survival. BMC biology. 15 (1), 113, (2017). [PubMed: 29183319]
13. Nicholls DG et al. Bioenergetic profile experiment using C2C12 myoblast cells. Journal of visualized experiments : JoVE. 10.3791/2511 (46), (2010).
14. Lobanova ES et al. Transducin translocation in rods is triggered by saturation of the GTPase-activating complex. The Journal of neuroscience : the official journal of the Society for Neuroscience. 27 (5), 1151–1160, (2007). [PubMed: 17267570]
15. Winkler BS The electroretinogram of the isolated rat retina. Vision research. 12 (6), 1183–1198, (1972). [PubMed: 5043568]
16. Jastroch M, Divakaruni AS, Mookerjee S, Treberg JR & Brand MD Mitochondrial proton and electron leaks. Essays in biochemistry. 47 53–67, (2010). [PubMed: 20533900]
17. Divakaruni AS, Paradyse A, Ferrick DA, Murphy AN & Jastroch M Analysis and interpretation of microplate-based oxygen consumption and pH data. Methods in enzymology. 547 309–354, (2014). [PubMed: 25416364]
18. Du J et al. Phototransduction Influences Metabolic Flux and Nucleotide Metabolism in Mouse Retina. The Journal of biological chemistry. 291 (9), 4698–4710, (2016). [PubMed: 26677218]

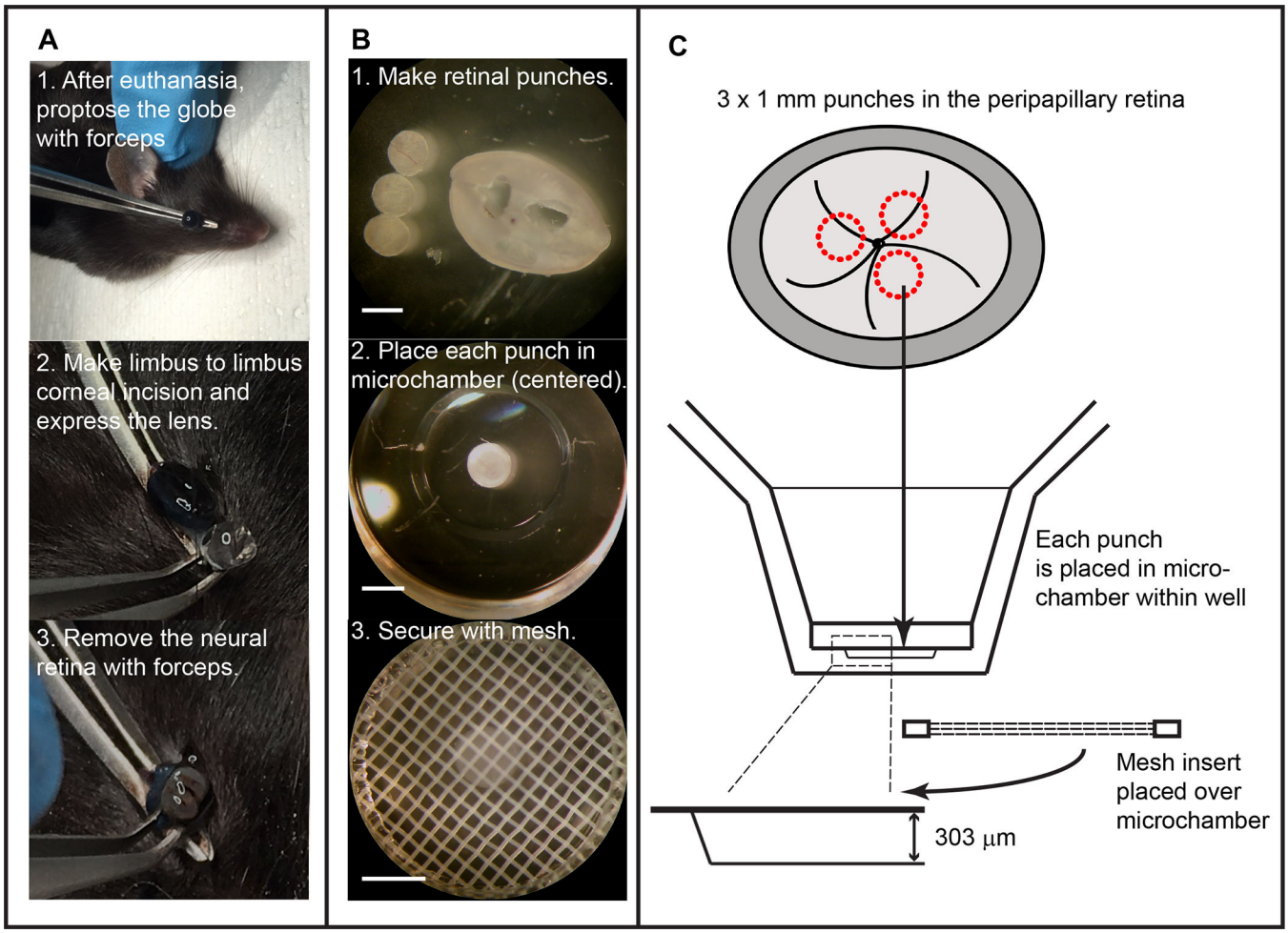

Figure 1:

Isolation of retinal explant and setup into the extracellular flux analyzer. (A) Isolation of the neural retina *in situ* by applying propulsive force on globe with forceps, incising the cornea, and removing retina after discarding lens and anterior hyaloid membranes. (B) Preparation of tissue for flux recording with retinal punch creation, placement of individual punches into islet capture microplate, and use of a mesh insert to minimize tissue movement with microchambers (Scale bars = 1 mm). (C) Schematic, derived from manufacturer-provided data, showing procedure outline and demonstrating height of the microchamber is adequate to accommodate the murine retina.

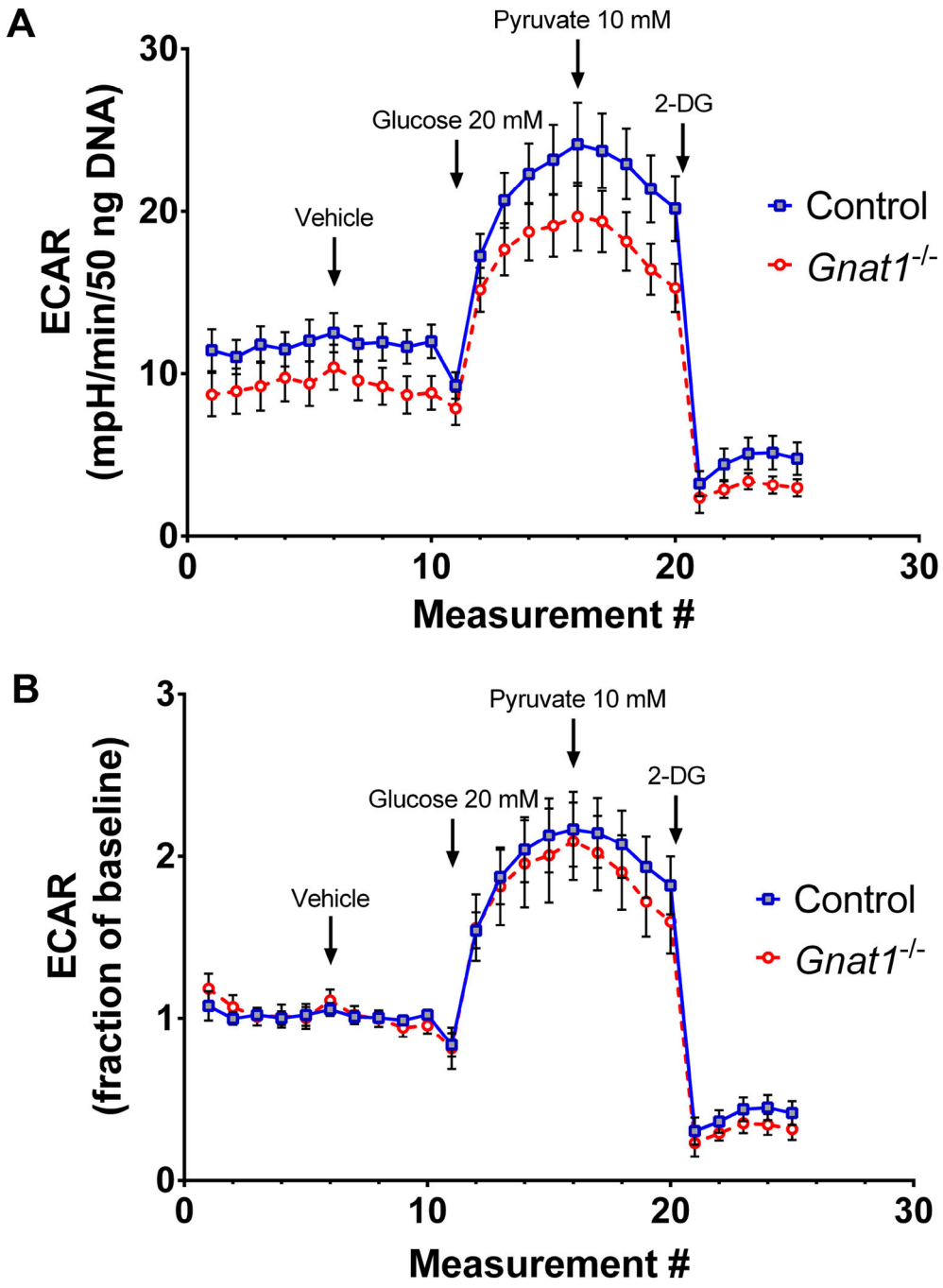

Figure 2:

Mitochondrial stress analysis using explanted retina from 8 week-old animals. (A) Averaged tracings with SEM, normalized to DNA content of the tissue, from an experiment optimized for oxygen consumption recordings, comparing *transducin* knockout animals (*Gnat1*$^{-/-}$) to wild type controls. (B) Same experiment with data transformed such that baseline recordings are set as the reference.

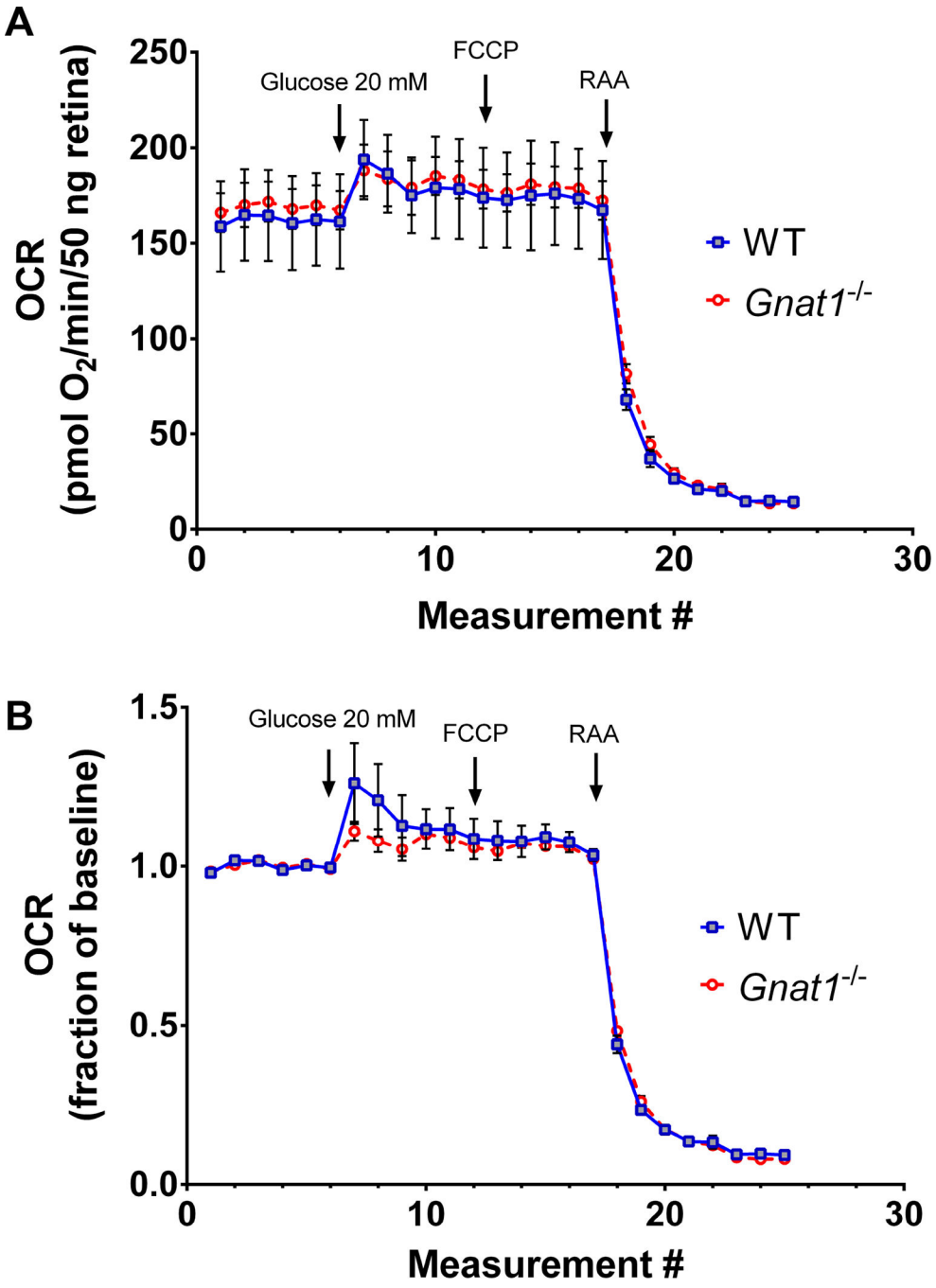

Figure 3:

Analysis of glycolytic rate using explanted retina from 8-week old animals. (A) Averaged, DNA content-normalized, tracings from an experiment optimized for acid efflux recordings comparing *transducin* knockout animals (*Gnat1*$^{-/-}$) to wild type controls. (B) Data from the same experiment normalized to baseline recordings. Traces show mean +/− SEM.

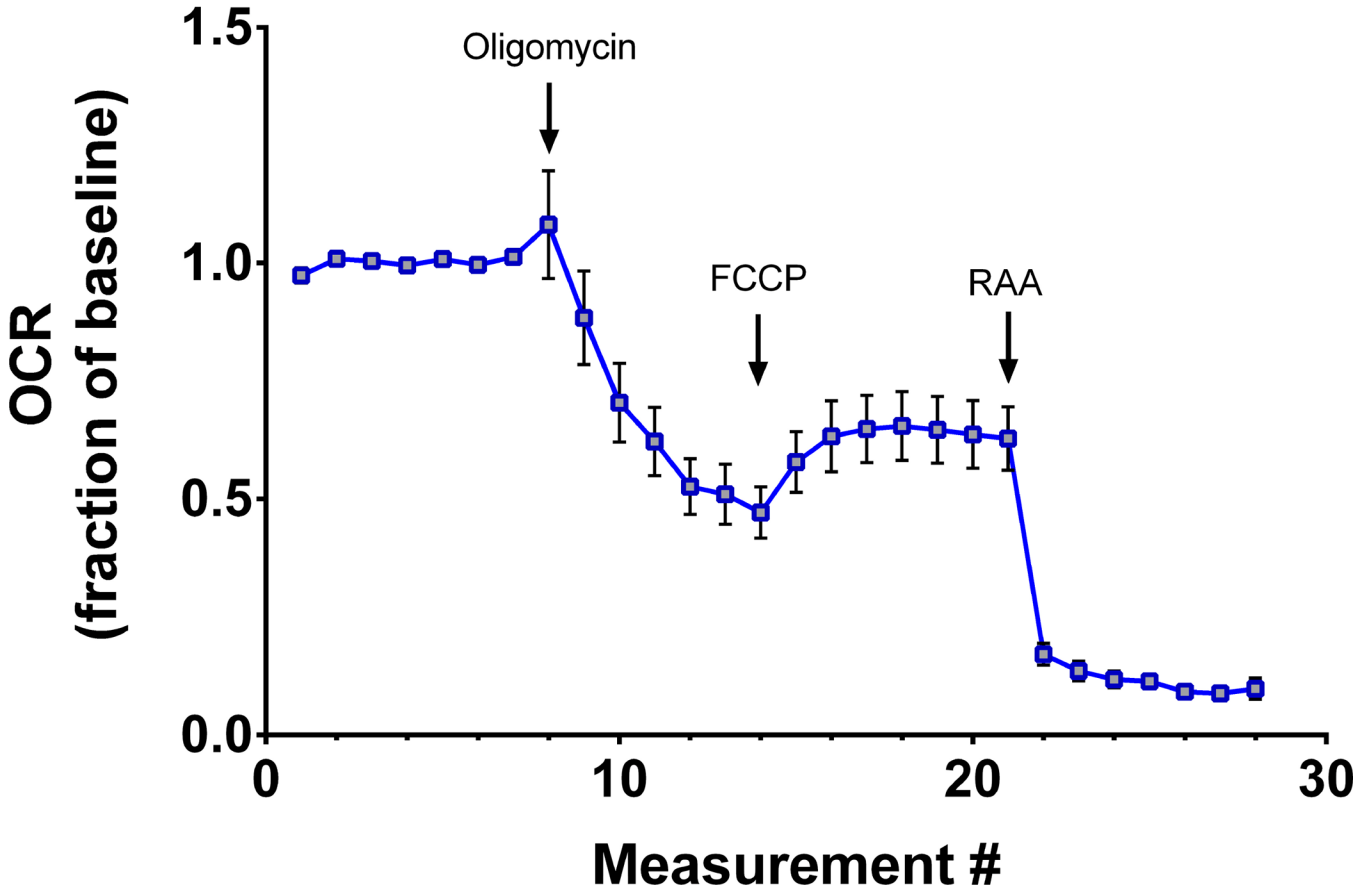

Figure 4:

Irreversible effects of oligomycin on retinal respiratory rates. In acutely prepared retinal explants from 8 week-old C57BL/6J mice, oligomycin treatment reduces the maximal OCR induced by subsequent addition of FCCP. Traces show mean +/− SEM.

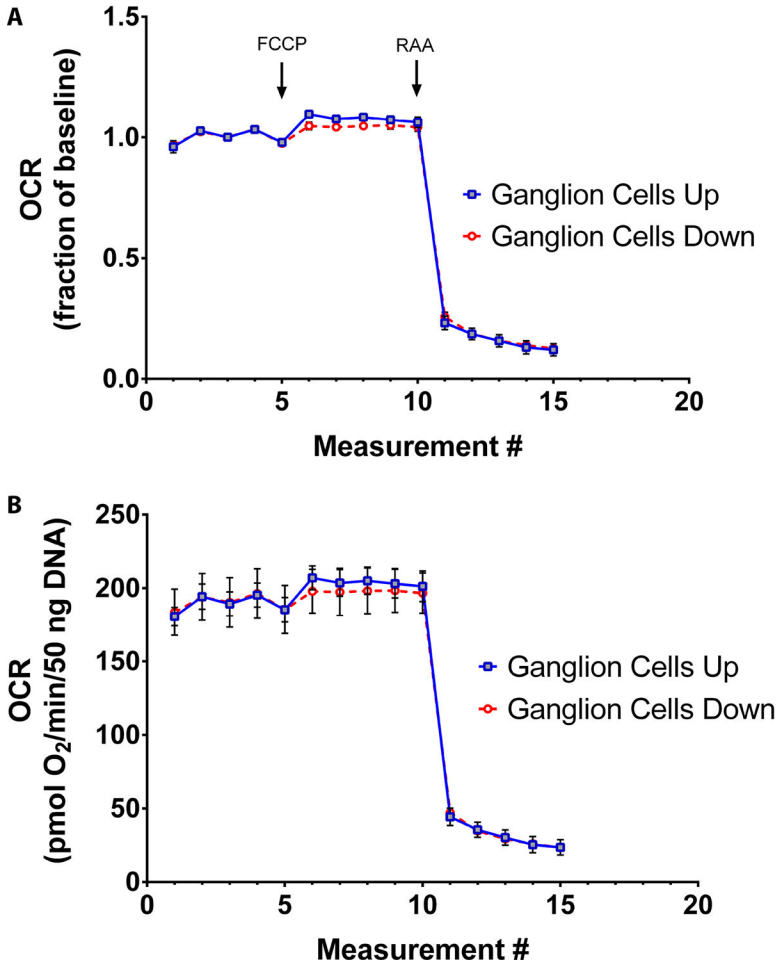

Figure 5:

Effects of tissue positioning on OCR measurement. Retinal tissues from 8 week-old C57BL/6J mice were placed in wells with ganglion cells facing toward the sensor (Ganglion Cells Up) or away from the sensor (Ganglion Cells Down). Between groups, similar extracellular flux recordings are observed in terms of (A) respiratory capacity relative to baseline or (B) in terms of absolute quantification. Traces show mean +/− SEM.